



Noise generation by a supersonic leading edge. Part 2: examples of two-dimensional sound fields

C.J. Powles

Department of Mathematics, Keele University, Staffordshire ST5 5BG, UK

Received 7 February 2002; accepted 5 August 2003

Abstract

Formulae for the calculation of the sound fields generated by the interaction between a flat-plate semi-infinite aerofoil and a convected vortical gust in a supersonic mean flow have been developed in part 1. Now the special case of two-dimensional sound fields is considered, and specific examples are given. The examples include a periodic gust, transient gusts, and the problem of a line vortex sweeping past the aerofoil. Study of the resulting fields gives insight into the general behaviour which may be expected. The two-dimensional results are important in the study of complicated three-dimensional fields, as the near-fields often contain a region in which the field is two dimensional.

© 2003 Elsevier Ltd. All rights reserved.

1. Introduction

In Part 1 [1], a set of general formulae for the sound fields generated by the interaction between a supersonic semi-infinite flat-plate aerofoil and a vortical gust were derived. These formulae are valid for fully three-dimensional sound fields, generated by arbitrary gusts, but are of a rather complicated form. Corresponding subsonic results have been derived by Chapman [2], with examples (some similar to the ones considered here) in Ref. [3]. The aim of the present paper is to derive a somewhat simpler result from the general supersonic formulae, that will be valid for the case of two-dimensional sound fields, which are generated by gusts with a shape independent of the span direction. This simpler result will be applied to a variety of such gusts, giving a number of examples of the types of sound fields which may be generated. Thus, a deeper understanding of the model and the effects of certain gust features is obtained. The near-fields of many three-dimensional fields often contain a region in which the field is two dimensional, and thus the results of this paper are important in the analysis of many complicated three-dimensional fields.

E-mail address: c.j.powles@maths.keele.ac.uk (C.J. Powles).

Many previous authors have considered the two-dimensional aerofoil–gust interaction problem. Much of this work is summarized in the book by Miles [4], but as was noted in part 1 this text is almost totally concerned with surface values of the pressure (or the velocity potential). This reflects the research interests of the time, with the prime concern being the calculations of the moments and forces acting on the aerofoil, and with very little interest in the generated acoustic field. For example, a well-known general two-dimensional result is quoted and utilized by Landahl [5], but this result gives values of the velocity potential only on the aerofoil surface. The result was originally derived by Garrick and Rubinow [6], who begin by considering the potential generated throughout the space by a point source. However, when they go on to derive the general result, they let the co-ordinate normal to the aerofoil surface take the value zero, so that again only surface values are given. Thus it appears that no general two-dimensional result *for the acoustic field* exists in the literature. One important example of the calculation of a specific two-dimensional field does exist: Strang [7] gives the result for an aerofoil entering a sharp edged gust. His method of calculation is to model the aerofoil as a distribution of line sources which “switch on” as the gust sweeps past: while the resulting superposition integral leads to the correct solution, it masks the fact that the noise source is actually the leading edge rather than the entire plate surface.

The analysis in this paper begins in Section 2, where the specific result for two-dimensional sound fields is derived from the results of part 1. In Section 3, examples of the sound fields due to five specific gusts are derived, and discussed in some detail. The first four gusts considered are described by a velocity component normal to the plate surface. The first of these is a single-frequency gust, which periodic disturbance leads to an interesting interference pattern in the pressure field. The second gust is described by a Dirac delta function, and so is somewhat of a mathematical abstraction. Such a gust can however be described in generalized function theory as the limit of certain types of gust, and as such the field derived has properties which are of interest for comparing to more physically realizable gusts. The third field considered is that due to a gust which might be described as “top-hat”: it has sharp edges, i.e., a sudden beginning and end, and is of constant magnitude between these ends. The fourth field is then a gust which is likewise localized, but with a smooth velocity profile: the profile chosen is a Gaussian function. As a final example, the case of a line-vortex sweeping past the plate is considered. Finally in Section 4, a general discussion of the results is given.

2. The general results

The general physical system in question is shown in Fig. 1. A flat-plate aerofoil of infinite span and semi-infinite chord is located in the plane $y = 0$, $x > 0$. A system of wind tunnel co-ordinates is chosen with the z -axis lying along the leading edge. The entire fluid (taken to be inviscid) has a uniform mean flow speed U in the positive x -direction, so that the angle of attack of the aerofoil is zero. Then the x -, y - and z -directions may be described as streamwise, vertical and spanwise, respectively. The Mach number of the fluid is defined by $M = U/c_0$, where c_0 is the speed of sound in the fluid. A supersonic mean flow is assumed, and so throughout the analysis $M > 1$.

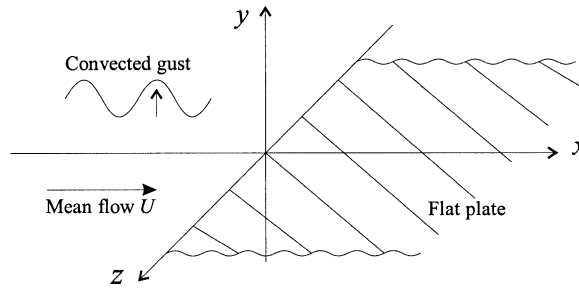


Fig. 1. Co-ordinate system for the study of a flat-plate aerofoil at rest in a mean flow of speed U , with a convected gust present in the fluid. The aerofoil occupies the plane $y = 0, x \geq 0$.

It is convenient to introduce a set of Doppler adjusted co-ordinates defined by

$$\bar{x} = x/(M^2 - 1), \quad \bar{y} = y/(M^2 - 1)^{1/2}, \quad \bar{z} = z/(M^2 - 1)^{1/2}. \tag{1}$$

These account for all the Doppler factors which appear in the subsequent formulae, and also allow the equations for Mach cones and wedges to be expressed in a compact form.

The gust is a vortical disturbance which is convected with the mean fluid flow, and it is assumed that all the disturbances are small enough that the linear theory may be applied. In the linear theory, the incoming vorticity field only interacts with the acoustic pressure field at the surfaces of the plate, where the two fields must combine in such a way as to satisfy a condition of zero fluid velocity normal to the surface. Thus, the physical situation is that the incoming vorticity field is associated with some solenoidal velocity field in the fluid, which on striking the plate leads to the generation of an irrotational acoustic particle velocity, associated with a pressure field. Then in order to calculate the form of the generated pressure field, the magnitude of the vortical velocity field at the plate surface must be known. In the linear theory, this field is frozen, only convecting with the mean flow: thus it must be some function of $t - x/U$. The function $f(t - x/U, z)$ is thus defined as the y component of the gust velocity in the plane $y = 0$.

In Part 1, the acoustic pressure and velocity are defined in terms of a potential, which must satisfy the convected wave equation. To specify unique and meaningful solutions, the zero normal velocity condition on the plate surface is combined with a condition of zero acoustic velocity upstream of the plate (due to the supersonic flow convecting sound downstream) and conditions of causality and radiation. The resulting boundary value problem is solved by the application of Fourier transforms, and the resulting inversion integral is partially inverted using complex variable techniques. The result is a double integral formula for the acoustic pressure, is given in terms of the transform of the gust function $f(t - x/U, z)$, which is defined by

$$F(\omega, m) = \int_{-\infty}^{\infty} \int_{-\infty}^{\infty} f(t, z) e^{i(\omega t - mz)} dt dz. \tag{2}$$

This is actually the transform of the gust profile as seen at the leading edge, where all of the sound is generated.

The general expression for the acoustic pressure field is discontinuous across the two half-planes described by the equation $\bar{x} = |\bar{y}|$. In the unadjusted co-ordinate space these meet the plate at the Mach angle $\mu = \tan^{-1}((M^2 - 1)^{-1/2}) = \sin^{-1}(1/M)$. These planes are the boundary of the Mach

wedge: outside of this wedge, i.e., in the region $\bar{x} < |\bar{y}|$, the pressure field is identically zero, since all of the sound generated is swept downstream at a greater velocity than that at which the field spreads. Inside the wedge, the pressure is given by the double integral

$$p(x, y, z, t) = \frac{-\rho_0 M c_0 \operatorname{sgn}(y)}{(2\pi)^2 (M^2 - 1)^{1/2}} \int_{-\infty}^{\infty} \int_{-\infty}^{\infty} F(\omega, m) e^{-i\omega(t - M\bar{x}/c_0)} e^{imz} \times J_0 \left(\left\{ \omega^2/c_0^2 + m^2(M^2 - 1) \right\}^{1/2} (\bar{x}^2 - \bar{y}^2)^{1/2} \right) dm d\omega, \quad (3)$$

where J_0 is the Bessel function of the first type of order zero. When one evaluates this integral for specific gusts, the causality condition dictates that the integration contour in the complex ω -plane should run above any singularities.

The above result is valid for arbitrary gusts, which can give rise to fully three-dimensional sound fields. A farfield expression for the case of three-dimensional sound fields is developed in part 1. In the current paper, the gusts of interest are those with velocity profiles which are independent of the span co-ordinate z , in which case two-dimensional sound fields are generated. A special case of the general result (3) is now derived for two-dimensional fields, by carrying out the integration with respect to the spanwise wavenumber m .

The form of the gusts of interest is $f(t - x/U, z) = f_0(t - x/U)$. From the general transform (2), the form of the gust transform $F(\omega, m)$ is

$$F(\omega, m) = \int_{-\infty}^{\infty} f_0(t) e^{i\omega t} dt \int_{-\infty}^{\infty} e^{imz} dz = F_0(\omega) 2\pi \delta(m), \quad (4)$$

where $\delta(m)$ denotes a Dirac delta function and $F_0(\omega)$ is the Fourier transform of the gust, defined by

$$F_0(\omega) = \int_{-\infty}^{\infty} f_0(t) e^{i\omega t} dt. \quad (5)$$

The evaluation of the integral with respect to z in Eq. (4) is carried out using the theory of generalized functions. The above result is inserted into the general equation (3), and the presence of the delta function allows the m integral to be trivially evaluated, leaving a single integral for the two-dimensional pressure field:

$$p(x, y, t) = \frac{-\rho_0 M c_0 \operatorname{sgn}(y)}{2\pi (M^2 - 1)^{1/2}} \int_{-\infty}^{\infty} F_0(\omega) e^{-i\omega(t - M\bar{x}/c_0)} J_0 \left(\frac{\omega}{c_0} (\bar{x}^2 - \bar{y}^2)^{1/2} \right) d\omega. \quad (6)$$

The above integral is of a simpler form than the more general result (3), as it does not have the root of a quadratic within the Bessel function. Before applying this result to any examples, it is useful to define a new variable,

$$\bar{r}_h = (\bar{x}^2 - \bar{y}^2)^{1/2}, \quad (7)$$

which is of fundamental importance in supersonic problems. The level surfaces of the variable are hyperbolic (hence the subscript h to distinguish it from a normal radius) and for large x they asymptote to the Mach wedge $\bar{x} = |\bar{y}|$. In the following problems, the decay factors in the sound fields are often functions of \bar{r}_h . This variable is seen not only in the two-dimensional analysis considered here, but also in the evaluation of the field near the Mach wedge for three-dimensional examples (see for example Eq. (42) in Ref. [1]). Indeed, in several examples of physical interest, the

fields near the leading edge and the Mach wedge are largely two dimensional, which is one of the prime reasons for studying the two-dimensional case. A number of examples are now considered.

3. Examples

3.1. The single-frequency gust

The first example to be considered is the case of a single-frequency gust. Such a gust, at normal incidence to the leading edge, is widely studied in the literature concerning subsonic mean flow, and indeed the calculation of the field due to such a gust is viewed as a canonical problem. However, results for this basic gust in the supersonic case could not be found in the existing literature. The gust is of the form

$$f_0(t - x/U) = v_0 e^{i\omega_0(t-x/U)}, \quad (8)$$

where v_0 is a vertical velocity. In common with the scaling of the length in the y -direction defined in Eq. (1), a scaled velocity $\bar{v}_0 = v_0/(M^2 - 1)^{1/2}$ is defined. The scaled variables should account for all of the Doppler factors in the solution. The gust term (8) has Fourier transform

$$F_0(\omega) = 2\pi v_0 \delta(\omega - \omega_0), \quad (9)$$

which when inserted into the general pressure expression (6) gives an integral which may be trivially evaluated, due to the presence of the delta function. The resulting pressure perturbation is

$$p(x, y, t) = -\rho_0 M c_0 \bar{v}_0 \operatorname{sgn}(y) e^{-i\omega_0(t - M\bar{x}/c_0)} J_0((\omega_0/c_0)\bar{r}_h). \quad (10)$$

The complex exponential has an argument which emphasises the travelling nature of the resulting wave pattern, with a velocity $((M^2 - 1)/M)c_0$ in the downstream direction, independent of y . The Bessel function on the other hand gives the y dependence of the field, completely in terms of the hyperbolic variable \bar{r}_h . The decay of the acoustic field is as $\bar{r}_h^{-1/2}$ for large \bar{r}_h , while as $\bar{r}_h \rightarrow 0$ the Bessel function tends to a constant, so that the sound field near the Mach wedge is unattenuated. The pressure jump across the Mach wedge is a straightforward discontinuity, with no singularity. The form of the field is shown in Fig. 2a.

The complicated form of the sound field illustrated in Fig. 2a may be seen as an interference pattern: it is the result of the fact that within a supersonic flow, radiation emitted from the same point at different times will interfere. This is illustrated geometrically in Fig. 2b. All sound is generated at the leading edge. If the sound generated at the instant $t = t_1$ is considered, it will generate a circular wavefront, which expands at the speed of sound c_0 whilst being swept downstream at the mean flow speed Mc_0 . Likewise, the sound generated at the later time $t = t_2$ also generates an expanding circular wavefront which is swept downstream. Eventually, as is shown in the figure, these wavefronts will overlap, and there will be a single point at which they meet. However, since the source is constantly emitting, every point within the Mach wedge is just such a point where two wavefronts meet. This is a well-known phenomenon in the study of supersonic flows, and is familiar in a simple form in electromagnetism, in the study of Cherenkov radiation (see, for example, Ref. [8, Chapter 13]). The result is that in the present case where the source magnitude is oscillatory, an interference pattern is generated.

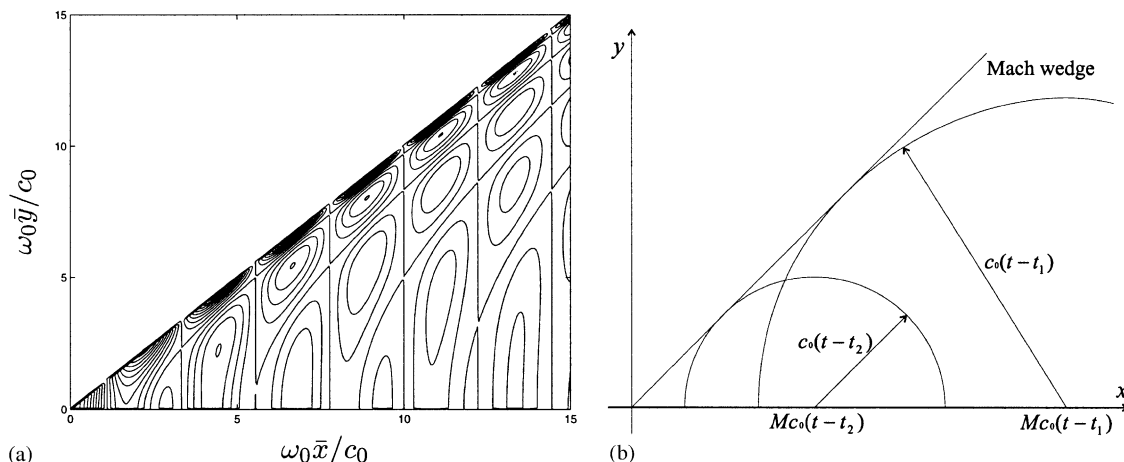


Fig. 2. (a) Pressure contours in the x, y plane. The abscissa represents $\omega_0 \bar{x} / c_0$, while the ordinate is $\omega_0 \bar{y} / c_0$. The Mach number is $\sqrt{2}$. (b) The dual influence effect in supersonic flow. Two wavefronts are seen to meet at a single point. See text for significance.

Letting $y \rightarrow 0^+$ in the pressure equation (10) gives the unsteady pressure on the upper aerofoil surface, which has in earlier papers tended to be of more interest than the radiated acoustic field. The explicit expression is

$$p(x, y, t) = -\rho_0 M c_0 \bar{v}_0 e^{-i\omega_0(t - M\bar{x}/c_0)} J_0((\omega_0/c_0)\bar{x}). \tag{11}$$

The pressure is the product of two waveforms: a purely harmonic waveform, i.e., the complex exponential, and the decaying Bessel function waveform. The result is the generation of what looks like a decaying modulated wave. The stationary envelope of this wave is provided by the Bessel function, which at large \bar{x} is of wavelength $2\pi c_0/\omega_0$ and decays as $\bar{x}^{-1/2}$. The non-decaying harmonic carrier wave component is of wavelength $2\pi c_0/(\omega_0 M)$. The difference in wavelength increases with Mach number, and the form of the wave is shown in Fig. 3a. As $M \rightarrow 1^+$, the wavelength of the carrier wave tends to that of the envelope, and the form of the composite is rather different (see Fig. 3b). The change is a result of the fact that the parts of the wavefronts that are trying to move upstream are in effect almost stationary in the wind-tunnel co-ordinates. Thus at larger Mach numbers there is a more rapidly modulated oscillation, while in the limit $M \rightarrow 1^+$ the components of the wave are nearly in phase, so that on large portions of the wing the pressure is almost all positive, and on other large portions the pressure is almost all negative. This can be seen in Fig. 3b, where over the range $10 < \omega_0 \bar{x} / c_0 < 17$ the oscillations are almost in phase and almost the entire pressure is positive, in stark contrast to the case in Fig. 3a.

3.2. The delta function gust

The velocity component of the gust is described by a Dirac delta function, and thus is a mathematical abstraction, which may be considered as a certain limit of very thin gusts. A time parameter τ is introduced in order to ensure the correct units. Then

$$f_0(t - x/U) = v_0 \delta((t - x/U)/\tau), \tag{12}$$

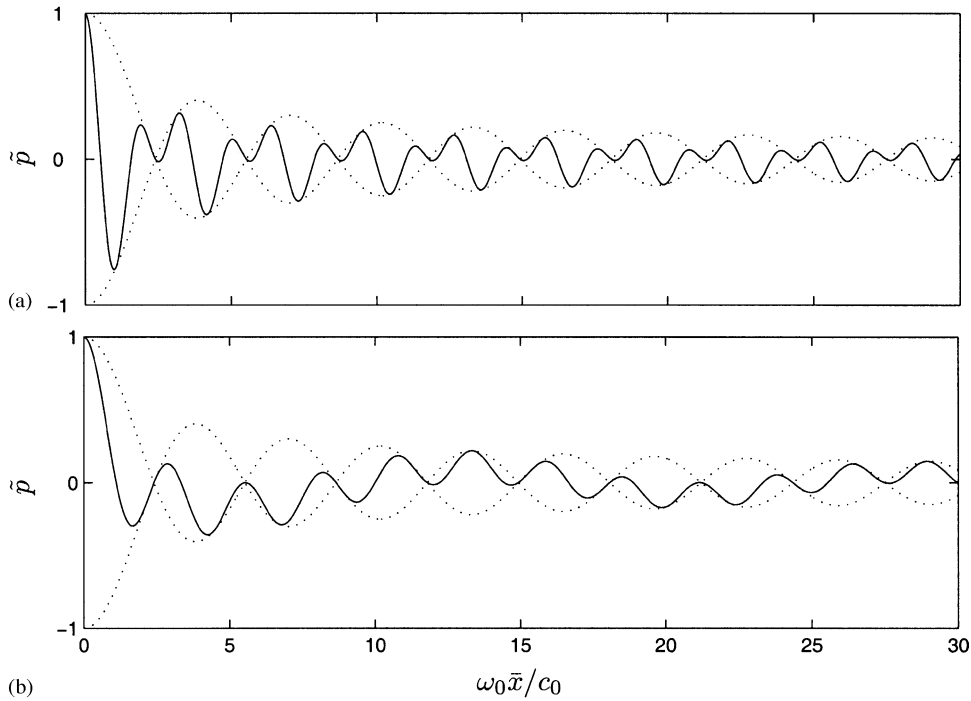


Fig. 3. The pressure wave pattern on the aerofoil at a fixed time for a single-frequency gust. The abscissa represents $\omega_0 \bar{x}/c_0$, while the ordinate is the normalized pressure. The dotted lines show the envelope wave, generated by the Bessel function. (a) For high Mach number, $M = 3$. (b) For low Mach number, $M = \sqrt{2}$.

which has Fourier transform

$$F_0(\omega) = v_0 \tau. \tag{13}$$

Applying the transform to the pressure integral (6), and utilizing the oddness and evenness of the imaginary and real parts, respectively, of the integrand, gives

$$p(x, y, t) = \frac{-\rho_0 M c_0 \bar{v}_0 \tau \operatorname{sgn}(y)}{\pi} \int_0^\infty \cos(\omega(t - M\bar{x}/c_0)) J_0\left(\frac{\omega}{c_0} \bar{r}_h\right) d\omega. \tag{14}$$

The above integral is a standard half-range transform of a Bessel function, as evaluated in Ref. [9, Eq. (1.12.1)], which takes the following values:

$$\int_0^\infty \cos(\omega a) J_0(\omega b) d\omega = \begin{cases} (b^2 - a^2)^{-1/2}, & a < b, \\ \infty, & a = b, \\ 0 & \text{otherwise.} \end{cases} \tag{15}$$

This result is applied to Eq. (14), and it is found that the condition for divergence may be arranged to the equation

$$(x - M c_0 t)^2 + y^2 = c_0^2 t^2. \tag{16}$$

This is an equation, in the non-Doppler-adjusted co-ordinates, for an expanding circle. The circle is generated at $t = 0$, when the gust strikes the leading edge, expands its radius at the speed of

sound c_0 , and its centre is swept downstream at the mean flow velocity Mc_0 . The integral evaluates to zero outside of the circle, as is required by causality, and takes on finite values within the circle. Then the pressure may be expressed in a single expression as

$$p(x, y, t) = \frac{-\rho_0 Mc_0 v_0 \operatorname{sgn}(y) c_0 \tau H(c_0^2 t^2 - (x - Mc_0 t)^2 - y^2)}{\pi (c_0^2 t^2 - (x - Mc_0 t)^2 - y^2)^{1/2}}, \quad (17)$$

where $H(\alpha)$ denotes a Heaviside unit-step function.

The pressure is singular on the circle, with a minimum at the centre. The singularity of the pressure on the circle is due to the highly singular nature of the gust. The acoustic pressure inside the circle, behind the initial wavefront generated at the origin, is due to the influence of points along the leading edge. The wavefront from any particular point on the leading edge is actually spreading spherically (whilst being convected). The extent of these combined wavefronts generates the cylindrical wavefront that is so apparent in Eq. (17), but effects are also felt within the cylinder. Then the pressure field of Eq. (17) is a classic example of the ‘tail’ effect of two-dimensional acoustics: although the source of the sound ends suddenly, there exists a lingering pressure field behind the cylindrical wavefront.

Pressure (17) is, excepting the $\operatorname{sgn}(y)$ term, exactly the pressure calculated by Strang [7] for a line source which emits a volume V per unit length per second as a delta function type pulse at $t = 0$, where in this case $V = -2Mv_0c_0\tau$. There is however no volume source present in the current problem. The explanation for what appears to be a volume source lies in Curle’s [10] extension to the acoustic analogy of Lighthill [11,12]. Curle’s specific contribution to the theory was to show that the effects of solid boundaries within a fluid may be modelled as dipoles, rather than the quadrupoles of Lighthill’s original theory. However, in the present problem, the supersonic flow means that the two sides of the aerofoil are independent, so that a distribution of poles is sufficient. Thus the generated field for the delta function gust is equivalent to a simple source term.

3.3. The top-hat gust

The top-hat function $H(\alpha, \alpha_1, \alpha_2)$ is defined such that it takes the value 1 for $\alpha_1 < \alpha < \alpha_2$, and the value zero elsewhere. Thus the gust is described by

$$f_0(t - x/U) = v_0 H((t - x/U)/\tau, -1, 1), \quad (18)$$

which has Fourier transform

$$F_0(\omega) = 2v_0 \sin(\omega\tau)/(\omega). \quad (19)$$

The variable τ is a time factor which describes the duration of the gust, which begins and ends suddenly. Substituting the transform into the pressure integral (10) gives

$$p(x, y, t) = \frac{-\rho_0 Mc_0 \bar{v}_0 \operatorname{sgn}(y)}{\pi} \int_{-\infty}^{\infty} \sin(\omega\tau) e^{-i\omega(t - M\bar{x}/c_0)} J_0\left(\frac{\omega}{c_0} \bar{r}_h\right) \frac{d\omega}{\omega}. \quad (20)$$

Rewriting the product of the sine and the complex exponential as the sum of single trigonometric functions, and utilizing the odd and even properties of the resulting integrands, the

integral in Eq. (20) may be expressed as the sum of two terms, denoted I_{\pm} , where

$$I_{\pm} = \int_0^{\infty} \sin(\omega(\tau \pm t \mp M\bar{x}/c_0))J_0\left(\frac{\omega}{c_0}\bar{r}_h\right)\frac{d\omega}{\omega}. \tag{21}$$

This, like integral (15), is a standard transform, and is evaluated in Ref. [13, Eq. (6.693.7)]. Each of the integrals has three regions of validity, which combine to cover the whole of the region under the Mach wedge. The result is

$$\int_0^{\infty} \sin(\omega\beta)J_0(\omega)\frac{d\omega}{\omega} = \begin{cases} \pi/2, & \beta > 1, \\ \arcsin \beta, & |\beta| < 1, \\ -\pi/2, & \beta < -1. \end{cases} \tag{22}$$

In the proper variables, the condition $|\beta| = 1$ for the integrals I_{\pm} may be expressed in the form

$$(x - Mc_0(t \pm \tau))^2 + y^2 = c_0^2(t \pm \tau)^2. \tag{23}$$

These are reminiscent of Eq. (16), which described the wavefront generated by a delta function gust. They are in fact the equations for the cylindrical wavefronts generated by the initial and final interactions, respectively, between the gust and the leading edge. The sound field within these areas is described by an arcsin, while outside these regions the integrals evaluate to constants. Whether the factors are positive or negative depends on the signs of $t \pm \tau - M\bar{x}/c_0$, and within the Mach wedge it may be shown that this is equivalent to whether the observation position is upstream or downstream of the points where the cylindrical wavefronts contact the Mach wedge. Then the factors cancel in most of space, so that the causality condition is satisfied.

The field is split into several regions, within which different expressions for the pressure are valid. The regions are labelled numerically, and may be expressed as

$$p_{1,2} = \frac{-\rho_0 Mc_0 \bar{v}_0}{\pi} \operatorname{sgn}(y) \left[\frac{\pi}{2} \pm \arcsin \left(\frac{c_0(t \pm \tau) - M\bar{x}}{(\bar{x}^2 - \bar{y}^2)^{1/2}} \right) \right], \tag{24}$$

$$p_3 = -\rho_0 Mc_0 \bar{v}_0 \operatorname{sgn}(y), \tag{25}$$

$$p_4 = p_1 + p_2 - p_3. \tag{26}$$

The regions in space to which these formulae are applicable are sketched in Fig. 4, which shows a time series of the interaction between the gust and the plate, in which the regions are labelled by the numbers denoting the appropriate pressure expression. The gust initially strikes the leading edge at a time $t = -\tau$, which interaction generates a cylindrical wavefront. Within the cylinder the expression p_1 is valid, the argument of the arcsin being well defined here, and in the region upstream of the wavefront, under the wedge, the pressure is a constant, given by p_3 . At the time $t = \tau$, the trailing edge of the gust strikes the leading edge, generating another circular wavefront, within which the expression p_2 is valid. Upstream of this region, the pressure is once again zero. As time passes the initial and final wavefronts will grow to overlap, and in the region in which they do so, the expression p_4 is valid. As they overlap region 3 of constant pressure shifts up towards the Mach wedge, but maintains its constant value. Thus there exists a ‘‘pellet’’ of pressure which, in the linear model, propagates to the far field unattenuated. In region 4 between the wavefronts,

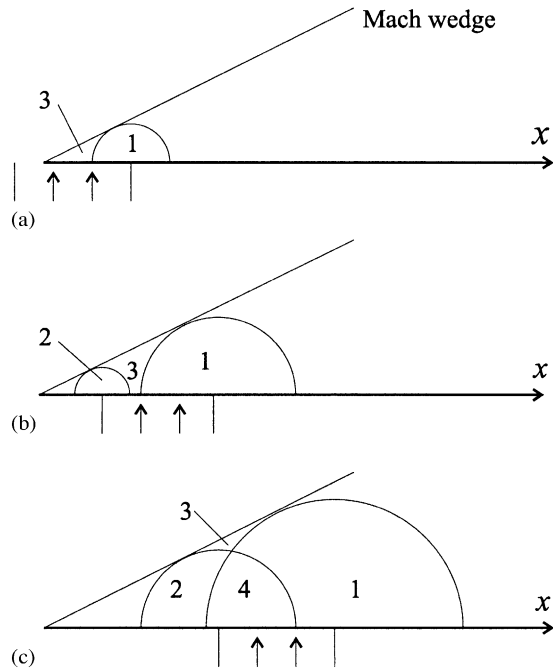


Fig. 4. Development of sound field due to a top-hat gust. (a) The gust is still striking the leading edge. There is a circular wavefront from the initial interaction. (b) The gust is past the leading edge. There are wavefronts from the initial and final interactions. (c) The important wavefronts have overlapped.

the pressure is now wholly due to the two-dimensional tail effects discussed in the delta function case.

Within the circular regions 1 and 2, before they interact, the pressure contours are ellipses, all of which pass through the points where the circles touch the Mach wedge. When the two circles overlap, the region between them develops a dip, and the borders of the overlap region are the peaks of the pressure field, excepting the unattenuated region 3, which has the highest pressure within the field. These properties are illustrated in Fig. 5a, which shows pressure contours in the x, y plane after sufficient time has elapsed for regions 1 and 2 to overlap. Within region 1, the pressure field is more spread out and the pressure generally lower than in the trailing region 2. The highest peak in the decaying part of the field then is at the border of regions 2 and 4.

Letting $y \rightarrow 0$ in the above expressions gives the pressure distribution on the plate. The distribution for a plate entering a sharp edged gust has been calculated by Strang [7, Eq. (4.3.1)], and his expression is in exact agreement to that found above when the rear edge of the gust has not yet reached the leading edge. The current work extends his results to consider the effect of leaving a sharp edged gust, and how these effects interact with the field generated by entering the gust. The region of constant pressure (the highest pressure in the field) disconnects from the plate, and the pressure on the plate develops a trough and decays, leading to the existence of two finite decaying pressure peaks on the plate. The general form of the pressure distribution on the plate is shown in Fig. 5b.

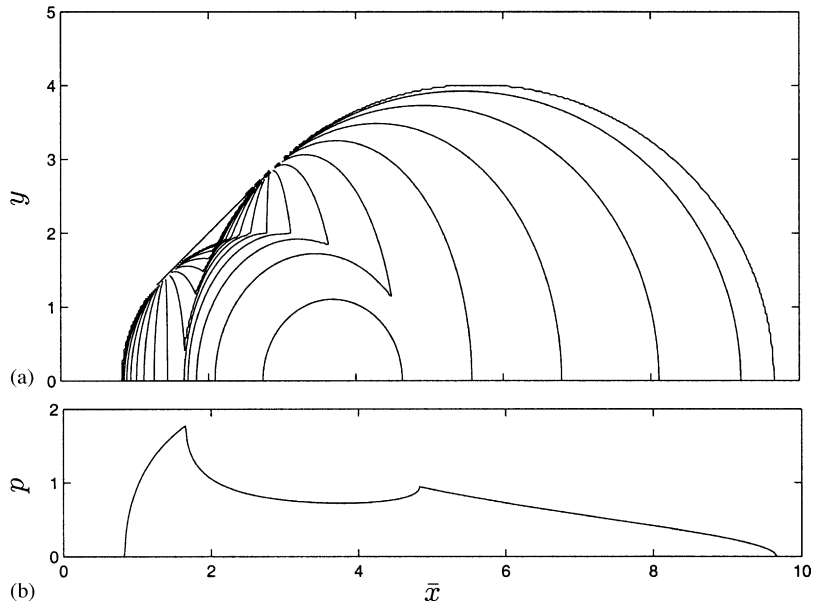


Fig. 5. The pressure field due to a top-hat gust. Parameter values are $\tau = 1$, $M = \sqrt{2}$, $t = 3$. (a) Pressure contours in the x, y plane. (b) Pressure on the upper aerofoil surface.

3.4. The Gaussian gust

Now a gust is considered which, like the previous example, is localized. A smooth velocity distribution is of interest: the sharp edges of the top-hat gust are replaced with a continuous function, and the flat top replaced by a curve. The gust is described by a Gaussian function

$$f_0(t - x/U) = v_0 e^{-((t-x/U)/\tau)^2/2}, \tag{27}$$

which has Fourier transform

$$F_0(t - x/U) = (2\pi)^{1/2} v_0 \tau e^{-(\omega\tau)^2/2}. \tag{28}$$

Substituting the transform into the pressure integral gives

$$p(x, y, t) = \frac{-\rho_0 M c_0 \bar{v}_0 \operatorname{sgn}(y) \tau}{(2\pi)^{1/2}} \int_{-\infty}^{\infty} e^{-(\omega\tau)^2/2} e^{-i\omega(t-M\bar{x}/c_0)} J_0\left(\frac{\omega}{c_0} \bar{r}_h\right) d\omega. \tag{29}$$

In this case no analytical expression for the pressure field could be found. A farfield expression has been developed, but is in the form of a sum of four terms, each of which is the product of a Gaussian and a Bessel function of fractional order, both of which have large arguments. As such it does not easily give much information about the form of the field. It is just as simple to evaluate the integral numerically and focus on discerning the important features from plots of the pressure contours.

The infinite integral (29) may be reduced to a finite integral suitable for rapid numerical evaluation by software such as Matlab. The Bessel function is replaced with a standard integral expression (a form of Eq. (9.1.18) from Abramowitz and Stegun [14]) in terms of a dummy

variable θ , the order of integration is reversed, and the integration with respect to ω is carried out. The standard integral is

$$J_0\left(\frac{\omega}{c_0} \bar{r}_h\right) = \frac{1}{2\pi} \int_0^{2\pi} e^{-i(\omega \bar{r}_h/c_0)\cos \theta} d\theta, \tag{30}$$

which, upon insertion into Eq. (29) and reversal of the order of integration gives

$$p(x, y, t) = \frac{-\rho_0 M c_0 \bar{v}_0 \tau \operatorname{sgn}(y)}{(2\pi)^{1/2}} \frac{1}{2\pi} \int_0^{2\pi} \int_{-\infty}^{\infty} e^{-(\omega\tau)^2/2} e^{-i\omega(t - M\bar{x}/c_0 + (\bar{r}_h/c_0)\cos \theta)} d\omega d\theta. \tag{31}$$

The above integral with respect to ω is seen to be a shifted Fourier inversion of the Gaussian function, which simply leads to another Gaussian, so that the final result is

$$p(x, y, t) = -\rho_0 M c_0 \bar{v}_0 \operatorname{sgn}(y) \frac{1}{2\pi} \int_0^{2\pi} \exp\left[-\frac{1}{2\tau^2} \left(t - \frac{M\bar{x}}{c_0} + \frac{\bar{r}_h}{c_0} \cos \theta\right)^2\right] d\theta. \tag{32}$$

This form of integral has two principal advantages over integral (29): the integration is carried out over a finite domain, and the integrand does not have the highly oscillatory nature of a Fourier inversion. Both of these facts mean that the integral is far easier to calculate numerically using simple computational packages.

An investigation of the above expression, using Matlab’s numerical integration routines, quickly reveals the general features of the pressure field. An example of the form of the pressure field is given in Fig. 6, in which Fig. 6a gives a contour plot of pressure in the x, y -plane, and Fig. 6b gives the pressure at $y = 0^+$ as a function of x . A similarity to the contours for the top hat

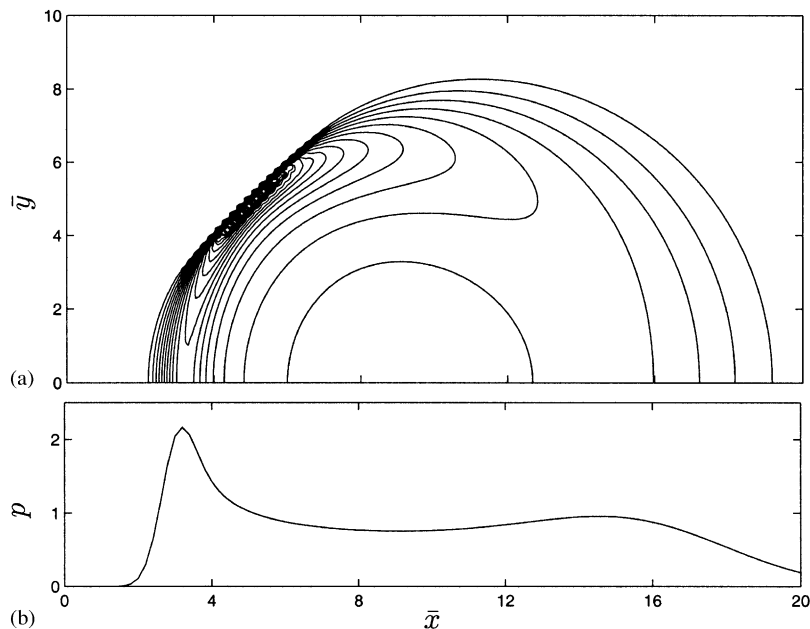


Fig. 6. The pressure field due to a Gaussian gust. Parameter values are $\tau = 1$, $M = \sqrt{2}$, $t = 7$. (a) Pressure contours in the x, y plane. (b) Pressure on the upper aerofoil surface.

gust is noted. The principal sound pulses are generated around the time $t = 0$, and spread cylindrically. The pattern thus resembles that in Fig. 5, as one pulse attempts to propagate upstream and another propagates downstream. In this case however the edges of the pulses are not sharp or well defined, and the peaks are smoothed. The forward pulse has the appearance of spreading and decaying more quickly, as for a top-hat gust, and a small high-pressure region exists near the Mach wedge, where previously the non-decaying high-pressure “pellet” was found. The field exists everywhere under the Mach wedge, as the gust has no sharp beginning or end. Thus considering a smooth gust removes some of the salient features of the sound field, but the general form is largely similar to that produced by the simple top-hat gust.

3.5. The line vortex

Rather than considering problems in which the gust is specified by a particular velocity component, as in the previous examples, it is interesting to consider a simple particular vorticity distribution. In principle, it is possible to obtain the required velocity component from an arbitrary vorticity distribution in terms of a triple integral (see, for example, Ref. [15]). Such an integral can then be Fourier transformed and inserted into the pressure integral (8), the integration order reversed and the m and ω integrals calculated, to leave a triple integral for the pressure in terms of the vorticity. However, even the two-dimensional case of the result is very unwieldy, and beyond the scope of the present paper. Here, a simple example shall be presented for which the required velocity component is trivially derived, and then the standard procedure is applied.

The problem to be considered is that of a line vortex sweeping past the aerofoil. It is assumed that the vortex is aligned parallel to the z -axis, so that the physical system is again two dimensional. The vortex has circulation Γ , and lies a vertical distance $y_0 > 0$ above the plane containing the aerofoil. In a low Mach number problem, it would be expected that the velocity induced by the interaction between the aerofoil and the plate would cause the vortex to move in the fluid, and this motion would have a serious effect on the form of the generated acoustic field (see Ref. [16] for a full discussion of this problem). However, given the high speed of the aerofoil in the supersonic problem, the induced motion of the vortex is likely to be very slight, especially near the leading edge where the noise is generated, so as long as Γ is not very large, the linear theory (in which the vortex simply sweeps past the aerofoil in a straight line) should give accurate results.

The azimuthal speed associated with a line vortex is simply $\Gamma/2\pi r$, where r is the radial distance from the vortex. If the vortex is assumed to be in the plane $x = 0$ at the instant $t = 0$, it can be shown by basic trigonometry that at that instant the required vertical velocity component in the plane $y = 0$ is $\Gamma x/2\pi(x^2 + y_0^2)$. Thus at an arbitrary time the velocity profile is given by

$$f_0(t - x/U) = \frac{\Gamma}{2\pi} \frac{x - Ut}{(x - Ut)^2 + y_0^2} = \frac{-\Gamma}{2\pi U} \frac{t - x/U}{(t - x/U)^2 + (y_0/U)^2}, \quad (33)$$

which takes into account the convection with the mean flow. The Fourier transform is

$$F_0(\omega) = (-i\Gamma/2U)e^{-|\omega|y_0/U} \operatorname{sgn}(\omega). \quad (34)$$

The transform is inserted into Eq. (6) for the pressure, and the resulting integral split into real and imaginary parts, the integrands of which are odd and even, respectively, so that the final expression is

$$p(x, y, t) = \frac{\rho_0 \Gamma \operatorname{sgn}(y)}{2\pi(M^2 - 1)^{1/2}} \int_0^\infty e^{-\omega y_0/U} \sin(\omega(t - M\bar{x}/c_0)) J_0\left(\frac{\omega}{c_0} \bar{r}_h\right) d\omega. \tag{35}$$

This integral might be expected in standard tables of transforms, but could not be found. The integral may be calculated in a general form, though the details of the analysis shall not be given here. The resulting expression is

$$\int_0^\infty J_0(\xi\alpha) e^{-\xi|\beta|} \sin(\xi\gamma) d\xi = \frac{\operatorname{sgn}(\gamma)}{\sqrt{2}} \left(\frac{((\alpha^2 + \beta^2 - \gamma^2)^2 + 4\beta^2\gamma^2)^{1/2} - (\alpha^2 + \beta^2 - \gamma^2)}{(\alpha^2 + \beta^2 - \gamma^2)^2 + 4\beta^2\gamma^2} \right)^{1/2}. \tag{36}$$

Upon application of Eq. (36) to the pressure equation, and after appropriate rearranging of the variables, one finds

$$p(x, y, t) = \frac{\rho_0 \Gamma \operatorname{sgn}(y)}{2\pi c_0 (M^2 - 1)} \left(\frac{(\Psi^2 + \Phi^2)^{1/2} - \Psi}{\Psi^2 + \Phi^2} \right)^{1/2}, \tag{37}$$

where

$$\Psi = c_0^2 t^2 - (x - M c_0 t)^2 - y^2 + \frac{(M^2 - 1)y_0^2}{M^2}, \tag{38}$$

$$\Phi = 2 \frac{y_0}{M} ((M^2 - 1)c_0 t - Mx). \tag{39}$$

It is difficult to interpret the form of the pressure field simply from the equations, but the form of the function Ψ is of interest. It is very similar to the circular terms found when dealing with previous transient gusts, as seen in Eqs. (16) and (23). Indeed, in the limit $y_0 \rightarrow 0$ it tends exactly to the circular variable defined for the delta function gust. The function Ψ then is indicative of the type of spreading of the sound field that is expected for a transient gust.

Contours of the sound field are plotted in Fig. 7a, the interpretation of which is aided by Fig. 7b, showing the pressure magnitude on the upper surface of the plate, i.e., at $y = 0^+$. The contours are for a time after the vortex has passed the leading edge of the aerofoil, so that the velocity component on the aerofoil is not single-signed. From Fig. 7b the pressure distribution on the aerofoil is composed of two humps, of opposite sign. The downstream hump has diffused and decayed more than the upstream hump, and in the field as a whole the pressure is composed of two parts. The largely cylindrical nature of the field is again seen, but here the downstream and upstream humps are of opposite sign, and in the large central circular region the pressure is very low indeed. The field is concentrated near the wedge, where it consists of a pair of high-pressure regions of opposite sign.

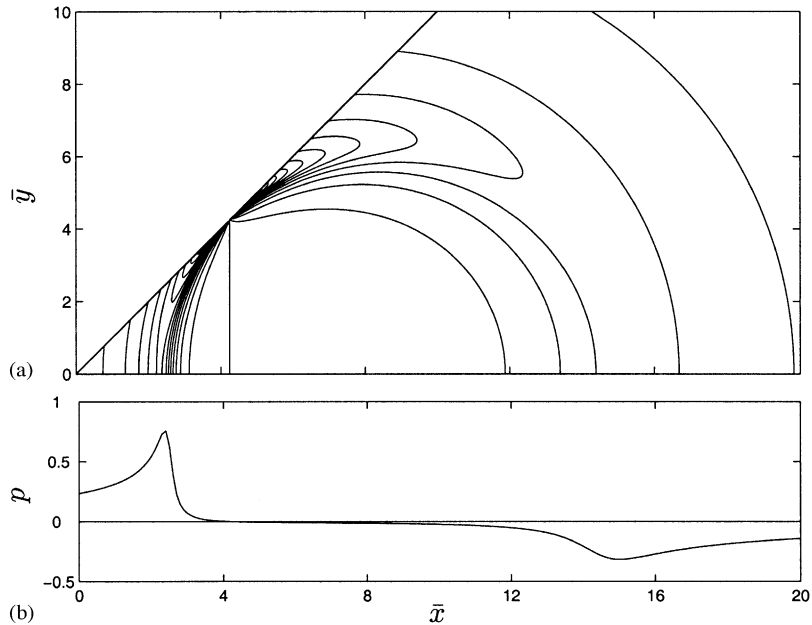


Fig. 7. The pressure field due to a line vortex sweeping past the aerofoil. Parameter values are $y_0 = 0.6$, $M = \sqrt{2}$, $t = 6$. (a) Pressure contours in the x, y plane. (b) Pressure on the upper aerofoil surface.

4. Discussion of results

A salient feature of all the sound fields that have been studied is the high-pressure regions near the Mach wedge. The existence of such regions may be explained mathematically by considering an expansion of the general pressure equation (6) near the Mach wedge. For a standard Taylor series expansion for small \bar{r}_h , the leading term p_1 will involve Eq. (6) evaluated at $\bar{r}_h = 0$, in which case the Bessel function is equal to the value 1, and the resulting integral is

$$p_1(x, y, t) = \frac{-\rho_0 M c_0 \operatorname{sgn}(y)}{2\pi(M^2 - 1)^{1/2}} \int_{-\infty}^{\infty} F_0(\omega) e^{-i\omega(t - M\bar{x}/c_0)} d\omega \tag{40}$$

$$= \frac{-\rho_0 M c_0 \operatorname{sgn}(y)}{(M^2 - 1)^{1/2}} f_0(t - M\bar{x}/c_0). \tag{41}$$

Eq. (41) is an application of the shifting theorem for Fourier transforms. The result is that in the Mach direction, the pressure perturbation is the same basic shape as the gust velocity, and propagates in the Mach direction unattenuated. This leads to the constant pressure “pellet” for the top-hat gust, and the high-pressure regions of opposite sign for the line vortex.

A range of examples has been considered. The canonical single-frequency gust is of considerable interest, displaying interference type behaviour, leading to modulated wave patterns on the aerofoil surface. The simple delta function gust naturally leads to a highly singular sound field, but the decay in the “tail” region of the field may be compared to that for the more realistic top-hat gust. This top-hat gust generates a highly structured sound field with definite regions of

causality, and the effects of considering a continuous localized distribution has been exhibited by study of the Gaussian gust. Finally, the physical problem of a line vortex sweeping past the blade has been considered. As a group, the examples lead to a fair understanding of the behaviour of the system.

An obvious next step in the work is to consider the three-dimensional effects which may occur. These will be wide and varied, but the great advantage of the two-dimensional work presented here is that most results may be analytically derived.

Acknowledgements

The author wishes to thank C.J. Chapman of Keele University for his patient guidance. This work was supported by a grant from the EPSRC.

References

- [1] C.J. Powles, Noise generation by a supersonic leading edge. Part 1: general theory, *Journal of Sound and Vibration* 276 (3–5) (2004) 837–852, [this issue](#).
- [2] C.J. Chapman, High-speed leading-edge noise, *Proceedings of the Royal Society of London, Series A* 459 (2003) 2131–2151.
- [3] C.J. Chapman, Some benchmark problems for computational aeroacoustics, *Journal of Sound and Vibration* 270 (2004) 495–508.
- [4] J.W. Miles, *The Potential Theory of Unsteady Supersonic Flow*, Cambridge University Press, Cambridge, 1959.
- [5] M.T. Landahl, *Unsteady Transonic Flow*, Pergamon Press, Oxford, 1961.
- [6] I.E. Garrick, S.I. Rubinow, Flutter and oscillating air-force calculations for an airfoil in a two-dimensional supersonic flow, NACA Report 846, 1946.
- [7] W.J. Strang, A physical theory of supersonic aerofoils in unsteady flow, *Proceedings of the Royal Society of London, Series A* 195 (1948) 245–264.
- [8] J.D. Jackson, *Classical Electrodynamics*, Wiley, New York, 1999.
- [9] A. Erdélyi, W. Magnus, F. Oberhettinger, F.G. Tricomi, *Tables of Integral Transforms*, McGraw Hill, New York, 1954.
- [10] N. Curle, The influence of solid boundaries upon aerodynamic sound, *Proceedings of the Royal Society of London, Series A* 231 (1955) 505–514.
- [11] M.J. Lighthill, On sound generated aerodynamically. 1. General theory, *Proceedings of the Royal Society of London, Series A* 211 (1952) 564–587.
- [12] M.J. Lighthill, On sound generated aerodynamically. 2. Turbulence as a source of sound, *Proceedings of the Royal Society of London, Series A* 222 (1954) 1–32.
- [13] I.S. Gradshteyn, I.M. Ryzhik, *Table of Integrals, Series, and Products*, 4th Edition, Academic Press, New York, 1980.
- [14] M. Abramowitz, I.A. Stegun, *Handbook of Mathematical Functions*, 5th Edition, National Bureau of Standards, Washington, 1966.
- [15] P.G. Saffman, *Vortex Dynamics*, Cambridge University Press, Cambridge, 1992.
- [16] M.S. Howe, *Theory of Vortex Sound*, Cambridge University Press, Cambridge, 2003.